

# Temporal and spatial variation of stable-isotope ratios and accumulation rates in the hinterland of Neumayer station, East Antarctica

Francisco FERNANDOY,<sup>1</sup> Hanno MEYER,<sup>1</sup> Hans OERTER,<sup>2</sup> Frank WILHELMS,<sup>2</sup> Wolfgang GRAF,<sup>3</sup> Jakob SCHWANDER<sup>4</sup>

<sup>1</sup>Alfred Wegener Institute for Polar and Marine Research, Telegrafenberg A43, D-14473 Potsdam, Germany  
E-mail: Francisco.Fernandoy@awi.de

<sup>2</sup>Alfred Wegener Institute for Polar and Marine Research, PO Box 120161, D-27515 Bremerhaven, Germany

<sup>3</sup>Helmholtz-Zentrum München, Ingolstaedter Landstrasse 1, D-85764 Neuherberg, Germany

<sup>4</sup>University of Bern, Sidlerstrasse 5, CH-3012 Bern, Switzerland

**ABSTRACT.** Four firn cores were retrieved in 2007 at two ridges in the area of the Ekström Ice Shelf, Dronning Maud Land, coastal East Antarctica, in order to investigate the recent regional climate variability and the potential for future extraction of an intermediate-depth core. Stable water-isotope analysis, tritium content and electrical conductivity were used to date the cores. For the period 1981–2006 a strong and significant correlation between the stable-isotope composition of firn cores in the hinterland and mean monthly air temperatures at Neumayer station was ( $r=0.54–0.71$ ). No atmospheric warming or cooling trend is inferred from our stable-isotope data for the period 1962–2006. The stable-isotope record of the ice/firn cores could expand well beyond the meteorological record of the region. No significant temporal variation of accumulation rates was detected. However, decreasing accumulation rates were found from coast to hinterland, as well as from east (Halvfarryggen) to west (Søråsen). The deuterium excess ( $d$ ) exhibits similar differences (higher  $d$  at Søråsen, lower  $d$  at Halvfarryggen), with a weak negative temporal trend on Halvfarryggen ( $0.04\text{‰ a}^{-1}$ ), probably implying increasing oceanic input. We conclude that Halvfarryggen acts as a natural barrier for moisture-carrying air masses circulating in the region from east to west.

## INTRODUCTION

The Antarctic ice provides one of the best palaeoclimate archives for the Holocene and large parts of the Pleistocene, as demonstrated for example by the ice cores of the European Project for Ice Coring in Antarctica (EPICA) at Dome C and in Dronning Maud Land (back to 800 ka) (EPICA Community Members, 2004, 2006; Jouzel and others, 2007). One of the four tasks formulated by the International Partnerships in Ice Core Sciences (IPICS) is to recover the oldest ice-core record in Antarctica (up to 1.2–1.5 Ma). In complementary work in the Northern Hemisphere, a new deep core is being extracted from the Greenland ice cap with the aim of recovering for the first time a complete record of the last interglacial period (Eem) from Greenland. Additionally, a bipolar network of intermediate-depth high temporal resolution cores dating back beyond the Last Glacial Maximum is promoted within the IPICS 40k array, as well as a worldwide IPICS 2k array initiative, thus including ice-core studies in high mountain regions at lower latitudes (Brook and others, 2006). This network will allow study of both the pre-industrial era and the most recent climate evolution, which is not covered properly by the existing meteorological and ice-core network. The work presented here was planned as a pre-site survey for an ice core contributing to the IPICS 40k array. Owing to higher than expected accumulation rates, we realized that an intermediate-depth ice core will most likely not cover 40 ka and thus will contribute to the IPICS 2k array.

In the last few years, it has been demonstrated that atmospheric warming in West Antarctica and some restricted coastal areas (Solomon and others, 2007; Steig and others, 2009) is most likely related to the release of industrial

gases into the atmosphere (Gillett and others, 2008). Based on meteorological and satellite observations, Steig and others (2009) concluded that West Antarctica showed air temperatures increasing by  $0.17 \pm 0.06^\circ\text{C} (10 \text{ a})^{-1}$  between 1957 and 2006, with a strong maritime influence. In contrast, East Antarctica exhibited a  $0.10 \pm 0.07^\circ\text{C} (10 \text{ a})^{-1}$  temperature rise and is dominated by more continental conditions. Other authors report that East Antarctica has been cooling slightly during the last half-century (Thompson and Solomon, 2002; Van den Broeke and Van Lipzig, 2004). This difference between East and West Antarctica was linked by Marshall and others (2006) and Marshall (2007) to the intensification of the Southern Annular Mode (SAM). Statistically significant warming trends have been observed only on the Antarctic Peninsula and in some restricted areas of the East Antarctic coast. In general, there is broad agreement that the Antarctic continent is subject to moderate warming only on the west side. This warming is in the range of the Southern Hemisphere's temperature increase of about  $0.08–0.12^\circ\text{C} (10 \text{ a})^{-1}$ , which probably began in the late 19th century, with increasing rates since the 1970s (Turner and others, 2005; Schneider and others, 2006; Chapman and Walsh, 2007; Monaghan and others, 2008; Steig and others, 2009).

In response to rising air and ocean temperatures, the mass balance of the Antarctic ice sheet reacts with a bimodal behaviour. Overall, West Antarctica is experiencing a clear negative mass balance of  $-48 \pm 14 \text{ km}^3 \text{ a}^{-1}$  (Rignot and Thomas, 2002). Extreme consequences on the dynamics of mass balance were observed at the northern Antarctic Peninsula. The disintegration of ice shelves along the

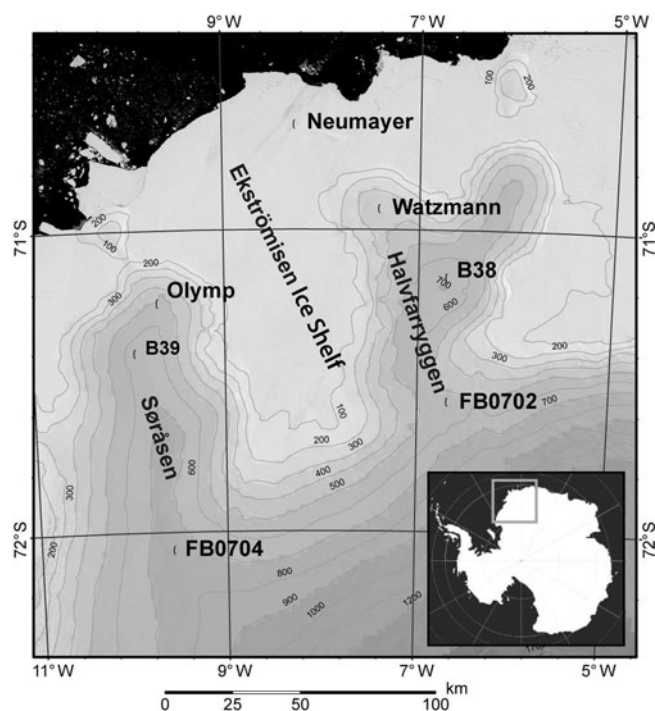


**Fig. 1.** Geographical location of the drilling sites. B38 and FB0702 are located on Halvfarryggen (east ridge); B39 and FB0704 on Søråsen (west ridge). Neumayer is the overwintering base on the Ekström Ice Shelf. Olymp and Watzmann are geophysical observatories. The shallow firn cores FB0701 and FB0703 were drilled at the same coordinates as FB0702 and B39, respectively. Contour intervals are 100 m. Elevations are given with respect to the World Geodetic System 1984 (WGS84). The inset map shows the location of the area under investigation (light grey) in Dronning Maud Land. The length scale is related to 71° S. The underlying image is from the Landsat Image Mosaic of Antarctica (LIMA) of the US Geological Service and the British Antarctic Survey (<http://lima.usgs.gov>). The digital elevation model is from Wesche and others (2009).

Antarctic Peninsula triggered an accelerated outflow of inland glaciers (Scambos and others, 2000; De Angelis and Skvarca, 2003; Rignot and others, 2004). These events are probably linked to the increase in sea-water temperature (Levitus and others, 2000; Robertson and others, 2002; Shepherd and others, 2004). The situation in East Antarctica has been widely discussed, mainly because it is impossible to make direct observations in such a vast territory. Rignot and Thomas (2002) could not confirm the sign of the mass balance ( $+22 \pm 23 \text{ km}^3 \text{ a}^{-1}$ ). The ice sheet seemed to stay close to a steady-state mass balance, with only local loss of mass especially in coastal regions (Rignot, 2006), or even to thicken (Davis and others, 2005). In contrast, new satellite observation techniques based on gravity measurements definitively demonstrate that the loss of mass in coastal regions is leading to a negative mass balance of East Antarctica (Chen and others, 2009). This evidence underlines the importance of making direct observations in coastal zones, where a large data gap still exists.

Many of the authors cited above agree that the future evolution of the ice sheet will be highly dependent on the reactions of ice shelves to increasing temperatures of ocean waters and the atmosphere. For this reason, more dense and accurate observations of accumulation rates and mass balance, especially in coastal zones, are needed. One of our principal aims is to reconstruct the recent climate

variability at a coastal site in East Antarctica. With this objective and in order to evaluate the potential of ice cores from coastal Dronning Maud Land for palaeoclimatic reconstruction, the regional variability of stable water isotopes has been examined.

We present new evidence supporting relatively stable conditions at least for the past 50 years in the hinterland of the German Neumayer station located in Dronning Maud Land, coastal East Antarctica (Fig. 1). We base our observations on detailed stable-isotope measurements of four firn cores retrieved in the austral summer of 2007.

## STUDY AREA AND BACKGROUND INFORMATION

In January 2007, a German–Swiss team drilled four firn cores on two ice ridges to the east (Halvfarryggen) and to the west (Søråsen) of the Ekström Ice Shelf (Fig. 1). The campaign was a pre-site survey to find a suitable location for intermediate deep coring in a coastal high-accumulation site, to be carried out in the framework of the IPICS 2k array project (Brook and others, 2006).

At Halvfarryggen, two firn cores, B38 (84 m deep) and FB0702 (42 m deep), were drilled. At Søråsen, B39 (78 m deep) and FB0704 (36 m deep) were retrieved. Additionally, 6 m deep firn cores FB0701 and FB0703 were drilled at the same positions as FB0702 and B39, respectively. High-resolution isotope measurements of these two shallow firn cores are used to fill a small gap in measurements of core FB0702 and to prove the reliability of stable-isotope records. Cores B04 and FB0202 (Schlosser and Oerter, 2002a), both drilled at Neumayer station, were also incorporated in our study. The geographical coordinates of all the drilling sites are given in Table 1.

The closest meteorological stations are located at the base Neumayer II (70°39' S, 8°15' W), which provides air-temperature data between 1992 and 2008, and the former base Georg-von-Neumayer (GvN; 70°37' S, 8°22' W), which provides data between 1981 and 1992. Both stations are hereafter referred to jointly as Neumayer station. Neumayer station is located at a distance of 80–164 km from the four drilling sites. According to König-Langlo and Loose (2007), the climatological conditions at Neumayer station are dominated by the circumpolar trough, with dominating easterly winds and characteristic katabatic winds during high-pressure events. Mean annual 2 m air temperature (MAAT) in the vicinity of Neumayer station shows a clear interannual variability, with an average temperature of  $-16.1^\circ\text{C}$  for the period 1982–2006. However, no significant temporal trend has been observed during this time-span. On a regular schedule, various glaciological observations have been carried out near the bases. Accumulation studies based on firn-core and snow-pit analyses as well as in situ observations (stake arrays) are in good agreement and give a rate of about  $360 \text{ kg m}^{-2} \text{ a}^{-1}$  for the period 1950–2000 (Schlosser and Oerter, 2002a).

The origin of the precipitation at the Ekström Ice Shelf was investigated by Schlosser and others (2004, 2008) by combining backward trajectory models and stable-isotope analyses of fresh-snow samples. Six main trajectory clusters were found to reach Neumayer station at the 850 hPa level (the assumed condensation level at Neumayer); the most frequent backwards trajectories originate over the Weddell Sea, closely followed by a cluster coming from the east along, or slightly north of, the coast. Other trajectories

**Table 1.** Dataset for cores B38, B39, FB0702 and FB0704 summarizing geographical characterization (coordinates and altitudes refer to WGS84), dating, accumulation rates and isotope composition for the common time-span 1962–2006. Measurements of  $\delta D$  (and  $\delta^{18}O$ ) were measured at 1.0 and 0.5 m resolution. The LMWLs shown at the bottom were calculated using a linear regression function of the correlation between  $\delta^{18}O$  and  $\delta D$

	B38	FB0702*	B39 <sup>†</sup>	FB0704	B04 <sup>‡</sup>	FB0202	FB0201 <sup>§</sup>	FB0203 <sup>§</sup>
Coordinates	71.16° S, 6.70° W	71.57° S, 6.67° W	71.41° S, 9.9° W	72.06° S, 9.56° W	70.62° S, 8.37° W	70.65° S, 8.25° W	71.21° S, 6.79° W	71.46° S, 9.86° W
Altitude	690 m a.s.l.	539 m a.s.l.	655 m a.s.l.	760 m a.s.l.	35 m a.s.l.	42 m a.s.l.	600 m a.s.l.	630 m a.s.l.
Depth	84 m	43 m	78.5 m	36 m	50.6 m	13 m	16 m	14 m
Age	1960–2007	1959–2007	1935–2007	1962–2007	1892–1981	1980–2001	1995–2001	1996–2001
Accumulation ( $kg\ m^{-2}\ a^{-1}$ )								
Mean	1257	547	818	489	352	329	1123	1105
Std dev.	347	168	238	128	91	109	214	214
Min.	501	257	405	326	172	146	752	703
Max.	2003	979	1467	835	572	627	1398	1278
$\delta^{18}O$ (‰)	(1.0 m res)	(0.5 m res)	(1.0 m res)	(0.5 m res)	(5.0 cm res)	(4.0 cm res)	(4.5 cm res)	(6.5 cm res)
Mean	-20.62	-24.25	-19.82	-22.76	-20.79	-20.26	-20.36	-20.12
Std dev.	2.16	2.29	1.63	2.04	2.63	3.13	3.48	3.79
Min.	-25.77	-29.54	-22.90	-26.40	-25.12	-27.97	-30.34	-31.09
Max.	-16.48	-17.04	-16.57	-19.23	-19.87	-12.71	-12.72	-14.07
n (samples)	78	77	54	70	1081	385	486	379
$\delta D$ ‰	(1.0 m res)	(0.5 m res)	(1.0 m res)	(0.5 m res)	(5.0 cm res)	(4.0 cm res)	(4.0 cm res)	(4.0 cm res)
Mean	-158.0	-188.6	-152.1	-175.9	-158.7	-156.6	-	-
Std dev.	16.6	18.3	13.0	16.4	21.8	25.5	-	-
Min.	-199.1	-231.0	-177.9	-204.6	-212.5	-218.5	-	-
Max.	-126.6	-134.0	-124.4	-147.5	-93.3	-94.4	-	-
n (samples)	>78	77	54	70	924	385	-	-
d (‰)	(1.0 m res)	(0.5 m res)	(1.0 m res)	(0.5 m res)	(5.0 cm res)	(4.0 cm res)	(4.0 cm res)	(4.0 cm res)
Mean	6.9	5.4	6.5	6.1	6.0	5.5	-	-
Std dev.	1.5	1.0	1.1	1.3	3.3	1.7	-	-
Min.	3.1	2.4	3.5	3.5	-6.1	-0.7	-	-
Max.	10.3	8.0	8.7	10.2	16.3	10.6	-	-
n (samples)	78	77	54	70	910	385	-	-
Co-isotope relation								
$\delta D$ vs $\delta^{18}O$ slope	7.64	7.99	7.91	8.01	8.04	8.07	-	-
$\delta D$ vs $\delta^{18}O$ intercept	-0.41	5.08	4.79	6.43	6.79	8.13	-	-

\*Same location as FB0701. <sup>†</sup>Same location as FB0703. <sup>‡</sup>Schlosser and others (2002a). <sup>§</sup>Masson-Delmotte and others (2008).

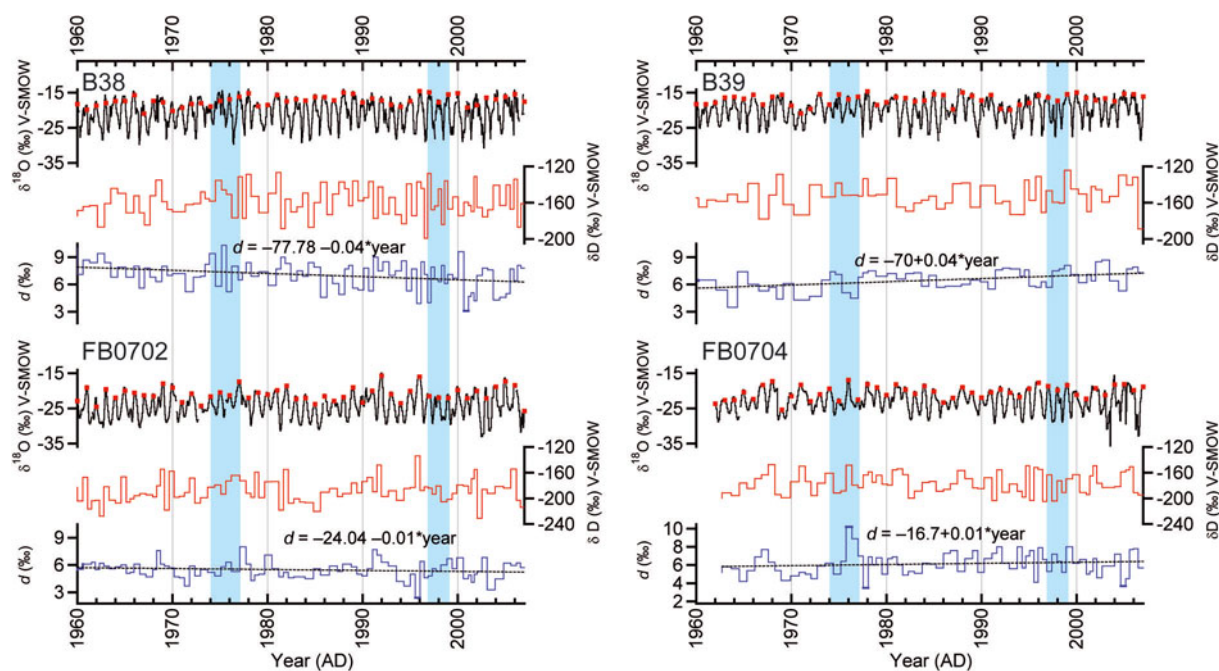


**Fig. 2.** Time series (1960–2007) of stable water isotopes from (a) cores B38 and FB0702 (Halvfarryggen) and (b) cores B39 and FB0704 (Søråsen). Black lines show  $\delta^{18}\text{O}$  data with high depth resolution (5–7 cm). The seasonal cycles are clearly visible for all cores and were used for the dating. Red dots indicate the austral summers defined as annual boundaries. The red lines show  $\delta\text{D}$  data on a lower depth resolution (1.0 and 0.5 m). At the bottom of each diagram (blue lines),  $d$  data at 1.0 m (B38 and B39) and 0.5 m (FB0702 and FB0704) resolution are shown. Dashed black lines represent linear regressions of  $d$  time series. A negative temporal trend for Halvfarryggen (B38 and FB0702) and a positive temporal trend for Søråsen (B39 and FB0704) were found. Only trends in B38 and B39 are statistically significant ( $p < 0.01$ ). Light blue bars represent the periods of prominent polynya events in the Weddell Sea region (1974–76 and 1997–98).

originate to the south of Neumayer station, in the South Atlantic Ocean (low latitude), in the Bellingshausen Sea and one between the Antarctic Peninsula and South America (Schlosser and others, 2004, 2008).

## METHODS

All firn cores were processed in the cold laboratory facilities of the Alfred Wegener Institute for Polar and Marine Research (AWI) in Bremerhaven. At first, the four cores were analysed using dielectric profiling (DEP) and  $\gamma$ -absorption (Wilhelms, 2000, 2005) at 5 mm resolution to determine electrical conductivity and density, respectively. Samples for stable water-isotope analysis were taken with depth resolutions of 1 m (B38 and B39) and 0.5 m (FB0702 and FB0704) for both  $\delta^{18}\text{O}$  and  $\delta\text{D}$ , and with higher resolutions of 7 cm (B38 and B39) and 5 cm (FB0702 and

FB0704) for  $\delta^{18}\text{O}$  only (Fig. 2). Stable-isotope measurements were performed with Finnigan-MAT Delta S mass spectrometers using the gas equilibration technique as described by Meyer and others (2000). The accuracy of this method is better than  $\pm 0.1\text{‰}$  for  $\delta^{18}\text{O}$  and  $\pm 0.8\text{‰}$  for  $\delta\text{D}$ .  $\delta^{18}\text{O}$  and  $\delta\text{D}$  values are given as deviation from the Vienna Standard Mean Ocean Water (V-SMOW) (‰). Tritium ( $^3\text{H}$ ) concentrations were measured along selected parts of cores B38 and B39 at a laboratory of the Helmholtz-Zentrum München, to assist the dating.

From stable-isotope measurements, different basic parameters were calculated to characterize the recent local and regional hydrological conditions in the study area. The global meteoric waterline (GMWL) is derived from the correlation between  $\delta^{18}\text{O}$  and  $\delta\text{D}$ , at global scale, given by the relation  $\delta\text{D} = 8\delta^{18}\text{O} + 10\text{‰}$  (Craig, 1961). At a regional scale this relation is expressed as the local meteoric

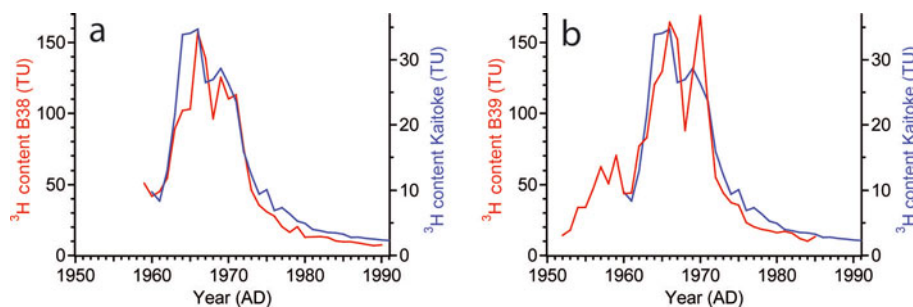


**Fig. 3.** Fit of the tritium profile (red curve) of firn cores (a) B38 and (b) B39 to the tritium profile of precipitation (blue curve) at Kaitoke, New Zealand. TU: tritium units. Tritium data of precipitation from International Atomic Energy Agency/World Meteorological Organization ([http://www-naweb.iaea.org/naweb/ih/IHS\\_resources\\_gnip.html](http://www-naweb.iaea.org/naweb/ih/IHS_resources_gnip.html)).

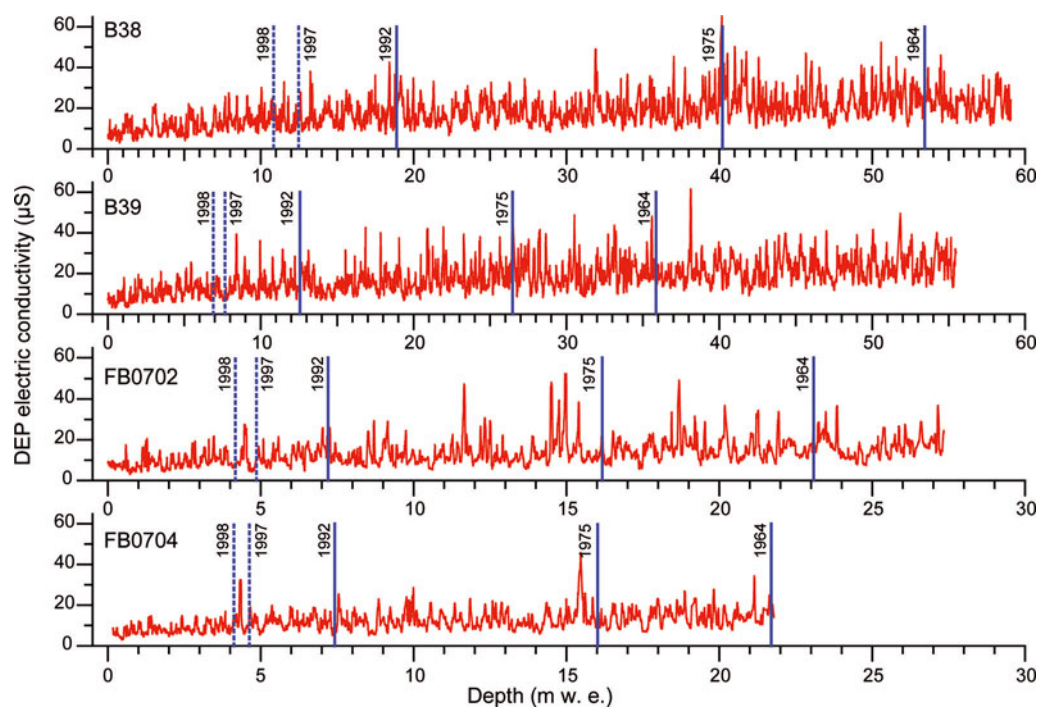


**Fig. 4.** DEP records for cores B38, B39, FB0702 and FB0704 plotted against depth. The years 1964 and 1992 for the known volcanic events of Mount Agung and Mount Pinatubo are marked as vertical bold blue lines; none of them can be recognized clearly in these DEP profiles. The third blue line marks the year 1975; elevated electric conductivity is observed in the corresponding depth of B38. Dashed blue lines show a peak visible only in both inland cores, observed between 1997 and 1998. DEP measurements were carried out at 5 mm resolution.

waterline (LMWL), which is influenced by local climatic and geographic conditions, as well as by input from secondary moisture sources, re-evaporation and/or sublimation (Merlivat and Jouzel, 1979; Clark and Fritz, 1997; Sharp, 2006). The second-order parameter deuterium excess,  $d = \delta D - 8\delta^{18}O$  (Dansgaard, 1964), is known to reflect conditions in the moisture source region.  $d$  depends on the sea surface temperature (SST), the wind speed and mainly on the relative humidity,  $h$ , at the source (Clark and Fritz, 1997; Sharp, 2006). Unlike  $\delta^{18}O$  and  $\delta D$ ,  $d$  generally does not vary during condensation of vapour masses (Merlivat and Jouzel, 1979; Sharp, 2006). Depletion of  $\delta^{18}O$  and  $\delta D$  will follow approximately a Rayleigh distillation model during condensation and precipitation of moisture (Jouzel and Merlivat, 1984). Therefore, the evolution of the  $\delta^{18}O$  and the  $\delta D$  content is related directly to air temperature, height, and distance from the source. The combination of both isotope systems allows us to study not only the precipitation process and its climatic implications, but also the origin and evolution of moisture masses.

## RESULTS

### Dating of the firn cores

The four firn cores were dated using annual-layer counting of seasonal variations of  $\delta^{18}O$ , assisted by DEP profiles and tritium measurements. The seasonal cycles of  $\delta^{18}O$  are generally easy to distinguish (Fig. 2). According to annual-layer counting, the oldest layers were deposited in 1935 (in core B39), 1959 (FB0702), 1960 (B38) and 1962 (FB0704). This dating was confirmed by the distribution in depth of the tritium content in cores B38 and B39 (Fig. 3; for details of the method used see Oerter and others, 1999).

The seasonal variations of the electrical conductivity (DEP) were used to check the layer counting (Fig. 4). However, no dominant peaks with volcanic-related events were found. Even the well-known acid depositions from the eruptions of Mount Pinatubo, Philippines, in 1991 (deposition in 1992) or Mount Agung, Indonesia, in 1963 (deposition in 1964), as mentioned by Hofstede and others (2004) and Traufetter and others (2004), could not be observed in our DEP profiles. However, a maximum in the DEP profiles of the coastal cores B38 and B39 was found and likely related to the year 1975. This peak could be linked to the occurrence of the Weddell polynya phenomenon during the winters of 1974–76 (Carsey, 1980). One of the most recent explanations for this peculiarity is the dynamic interaction of oceanic currents and the submarine topography in front of the Dronning Maud Land coast (Holland, 2001). The air–sea interaction contributed to an increase of the sea surface salinity (Moore and others, 2002). Therefore, this local moisture source could influence the dielectrical profiles of the cores in this period. In the hinterland cores FB0702 and FB0704, a similar maximum is observed slightly later (1976 or 1977). A second DEP peak (1997–98) coincides with another polynya event in the Weddell Sea (Ackley and others, 2001), but this last peak is not clearly visible in cores B38 and B39 (Fig. 4). As a consequence, the uncertainty of the dating was estimated to be less than  $\pm 2$  years for all cores. For B38 and B39, a dating uncertainty of  $\pm 1$  year is likely. In general, these examples show the difficulty in using DEP peaks for dating purposes in coastal areas with high snow accumulation rates. This is also due to the fact that DEP profiles are affected by high content of sea-salt components (Bertler and others, 2005), which may blur volcanic signals.

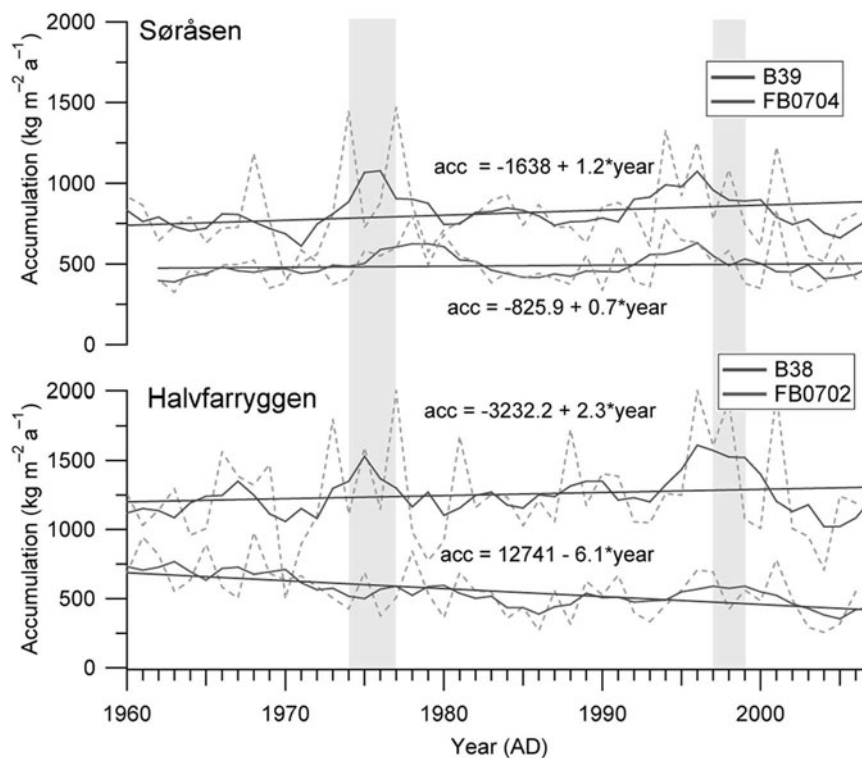


**Fig. 5.** Mean annual accumulation (acc) rates for cores B39, FB0704, B38 and FB0702 for the period 1960–2006. Annual accumulation rates (light grey dashed lines) were smoothed with a 5 year running mean function (red and blue bold lines). The cores closer to the coast (B38 and B39) are shown by blue lines, and the inland cores (FB0702 and FB0704) by red lines. Years of Weddell Sea polynya events are represented by the semi-transparent light blue bars (1974–76 and 1997–98).

## Accumulation

The accumulation map compiled by Rotschky and others (2007) gives an accumulation rate of  $170 \text{ kg m}^{-2} \text{ a}^{-1}$  for the area of Halvfarryggen, which originates from one shallow core (covering the period 1964–95) at the site of the Watzmann geophysical observatory (Fig. 1). However, our results show much higher accumulation rates for the time-span 1962–2006 for this area, with large spatial variation (Table 1). On the summit of Halvfarryggen (B38), an extraordinarily high accumulation rate of  $1257 \text{ kg m}^{-2} \text{ a}^{-1}$  was determined. Further to the south (FB0702), the accumulation rate decreases to  $547 \text{ kg m}^{-2} \text{ a}^{-1}$ . On the north of the western ridge of Søråsen (B39) an accumulation rate of  $818 \text{ kg m}^{-2} \text{ a}^{-1}$  has been determined, which decreases further to the south (FB0704) to  $489 \text{ kg m}^{-2} \text{ a}^{-1}$  (Fig. 5). From these values a negative gradient in accumulation rates is likely to be observed, not only from north to south but also from east to west. Although the shallow firn cores FB0201 and FB0203 (Table 1) (Masson-Delmotte and others, 2008), drilled in the vicinity of the Watzmann (Halvfarryggen) and Olymp (Søråsen) geophysical observatories, respectively, are both located closer to the coast, they show high accumulation rates of  $1123$  and  $1105 \text{ kg m}^{-2} \text{ a}^{-1}$ , respectively. These data do not seem to fit the regional pattern, however, as both cores are located on the slope of their respective ridges and could therefore be influenced by snowdrift. This finding underlines the problem of mapping the surface mass balance in coastal areas with complicated topography based on sporadic observations and with little geophysical (e.g. ground-penetrating radar) background information. Accumulation rate patterns can vary greatly over relatively short distances (Eisen and others, 2008).

Two prominent high-accumulation peaks are distinguishable in both northernmost cores (B38 and B39), the first between 1974 and 1977 and the second between 1996 and 1998. This feature is especially visible in the smoothed data (Fig. 5). The first high-accumulation event occurred during the period of the Weddell polynya and coincides with a high peak of DEP. During the Weddell polynya, a local increase in precipitation amount was detected (Moore and others, 2002). Elevated SST above the region free of sea ice causes more evaporation and cloud coverage, with a restricted moisture source producing locally increased precipitation rates. This feature is not observed in our inland cores, pointing to the local extent of the Weddell polynya effect. The second peak could be related to a more recent polynya event, as also shown by elevated conductivity profiles. However, this second high-accumulation peak begins at least 1 year before the polynya.

No firn cores except FB0702 show significant temporal accumulation trends. FB0702 shows a decreasing accumulation rate of  $6.1 \text{ kg m}^{-2} \text{ a}^{-1}$  ( $p < 0.01$ ). The topographical situation of core FB0702 from the eastern ridge could favour a local intensification of wind speed. Cold air masses originating on the higher plateau of Dronning Maud Land flow downslope and are slightly deflected to the west due to the Coriolis effects and the dominant regional wind regime (Van den Broeke and others, 2002; Van den Broeke and Van Lipzig, 2003). The wind reaching the east of Halvfarryggen is then channelled between the north summit of Halvfarryggen and the descending slope from the plateau of Dronning Maud Land. A similar phenomenon has been observed in other locations in Antarctica (Van den Broeke and others, 2002; Van den Broeke and Van Lipzig, 2003). Snowdrift is

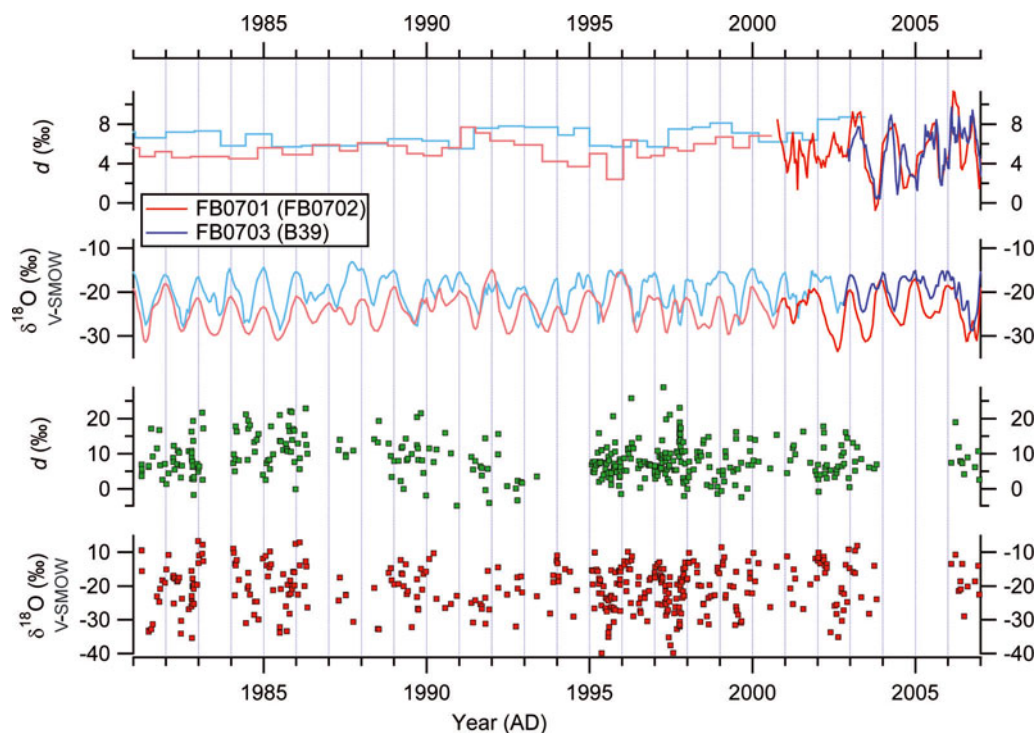


**Fig. 6.**  $\delta^{18}\text{O}$  and  $d$  data of fresh-snow samples (bottom) collected at Neumayer station in the period 1981–2006 and of the shallow firn cores FB0701 and FB0703 (top). Cores FB0701 (bold red line) and FB0703 (bold blue line) cover the time-spans 2000–07 and 2003–07, respectively. B39 and FB0702 are shown only for comparison in light colour lines (blue and red, respectively). These cores were drilled at the same position as FB0701 and FB0703, expanding the isotope record to the past. At the bottom (red and green squares), it can be observed that the sampling of fresh snow is not homogeneous in time and some time intervals are covered only weakly or not at all.

commonly reported from meteorological observations at Neumayer station. During these events the wind speed can reach up to  $30\text{ m s}^{-1}$  at surface level, mainly connected to easterly storms. Katabatic winds proceeding from the south are also reported (König-Langlo and Loose, 2007). Intensified snowdrift and/or erosion could therefore explain the decreasing accumulation rates in FB0702. This effect is not observed at the FB0704 location, so it is interpreted as a restricted local feature.

### $\delta^{18}\text{O}$ and $\delta\text{D}$

The firn cores B38 (690 m a.s.l.) and B39 (655 m a.s.l.) are located 81 km southeast and 110 km southwest of Neumayer

station, respectively. The respective mean annual  $\delta^{18}\text{O}$  values (accumulation-weighted) are  $-20.58\text{‰}$  for B38 and  $-19.96\text{‰}$  for B39 for 1960–2007. These values are close to the annual average  $\delta^{18}\text{O}$  for fresh snow collected at Neumayer station between 1981 and 2006 ( $\delta^{18}\text{O} = -20.49\text{‰}$ ) (Fig. 6). This is a substantial observation, which implies that despite the elevation difference of approximately 600 m between Neumayer station and the drill sites, no significant altitude effect is visible in the stable-isotope data.

The other two cores, located towards the interior of the continent, have more negative  $\delta^{18}\text{O}$  values:  $-24.23\text{‰}$  for FB0702 (539 m a.s.l.) and  $-22.74\text{‰}$  for FB0704 (760 m a.s.l.) (Table 1). The discrepancy of mean  $\delta^{18}\text{O}$  values between

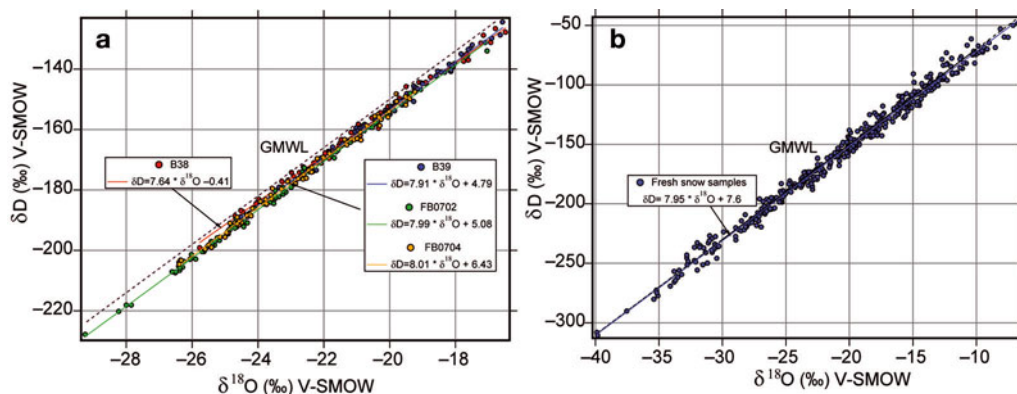


**Fig. 7.** Plots showing the relationship between  $\delta^{18}\text{O}$  and  $\delta\text{D}$  (1.0 and 0.5 m means) for (a) the four ice cores and (b) the fresh-snow samples from Neumayer station (1981–2006). Linear regressions of the co-isotope relationship of firn cores and snow samples were performed to be compared with the GMWL. Slopes in general agree well with the value 8 of the GMWL, except for core B38.

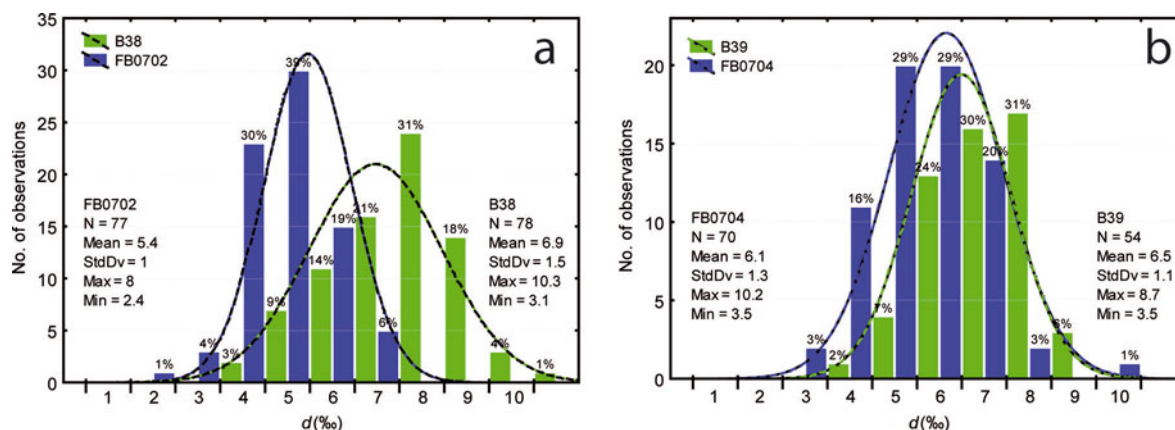


**Fig. 8.** Histograms showing the statistical  $d$  distribution for the four firn cores. (a) Cores from Halvfaryggen, where FB0702 shows slightly lower  $d$  values. (b) Cores from Søråsen. All cores were fitted to a normal distribution function (dashed curve).

these two cores cannot be explained by altitude or by continental effects. Potentially, a significant input of snow from higher elevations coming from the south of Halvfaryggen and transported by wind is the most likely explanation. However, no direct observation of this process (wind drift and/or erosion) has been made and these inferences are based only on our isotope data. Therefore, other phenomena cannot be discounted at this stage.

A gap in  $\delta D$  measurements in core B39 (uppermost 6 m) was filled with the isotope data from core FB0703, which was drilled at the same geographical coordinates as B39. FB0701, drilled near FB0702, was used to compare and verify the accuracy of the measurements. No important differences were detected (differences in  $\delta^{18}O$  are on average 0.1‰ and 0.3‰ for  $\delta D$ ). The  $\delta^{18}O$  and  $d$  values of both cores are plotted in Figure 6.

The co-isotope  $\delta^{18}O$  vs  $\delta D$  plot (Fig. 7) shows a good correspondence for the slopes of the firn cores and fresh snow. For all four firn cores, slopes are similar to the slope of the GMWL (Craig, 1961). This implies a strong oceanic influence and likely no secondary re-evaporation occurring in this area.

However, core B38 has a slightly lower slope of 7.6 and negative intercept ( $\delta D = -0.4‰$ ). In this case, if  $\delta^{18}O$  values greater than  $-18‰$  (related to warm summer temperatures) are removed, then the slope would increase to 7.7 and the intercept becomes positive ( $\delta D = 2‰$ ), probably demonstrating that conditions in the moisture source (or a shift of the source) occurred during the summer season.

The meteoric waterline for fresh snow from Neumayer station is very close to the GMWL, revealing that relative humidity,  $h$ , at the moisture source of the snow precipitating at the coastal zone is slightly higher than the global average (85%) (Clark and Fritz, 1997), whereas for the four hinterland cores the waterlines are displaced below the GMWL (lower intercepts). This displacement seems more likely to be related to post-depositional processes than to primary evaporation or moisture source conditions. This can be demonstrated observing the stable-isotope composition of shallow firn cores retrieved earlier near Neumayer station (e.g. B04 and FB0202; Schlosser and Oerter, 2002a) (Fig. 1; Table 1). All intercepts of these cores, except FB0202, are displaced to lower intercepts with respect to fresh snow. Consequently, the low intercepts are typical for coastal firn cores in the Ekström Ice Shelf region. Core FB0202 shows similar

intercept and slope to the snow samples in the co-isotope relation, but has a short time-span (19 years). In contrast, core B04 has a longer time-span (91 years) and a noticeable displacement with respect to snow values. This may suggest that post-depositional processes (diffusion and/or redistribution within the snow column) are acting slowly and preferentially over the deuterium isotope, since no important change in the slopes is detected.

The mean meteoric waterline calculated for the whole of Antarctica ( $\delta D = 7.75\delta^{18}O - 4.93$ ) by Masson-Delmotte and others (2008) agrees with the slope of our LMWL, but differs in the intercept, which is typical for coastal zones.

### Deuterium excess

The secondary parameter, deuterium excess ( $d = \delta D - 8\delta^{18}O$ ) of precipitation, is directly linked to the relative humidity ( $h$ ), SST and wind-speed conditions at the moisture source (Dansgaard, 1964; Clark and Fritz, 1997). Therefore, it can be used as a tool to distinguish between different source regions or changes in evaporation conditions in a stationary moisture source. Mean  $d$  values for the firn cores vary from 5.4‰ (FB0702) to 6.9‰ (B38) (Table 1; Fig. 8), which is well below the mean value of 8.6‰ for fresh-snow samples at Neumayer station (Table 2). These differences in  $d$  values between fresh snow and firn cores could either reflect the influence of different moisture sources (different  $h$  and/or SST from those of the fresh snow) or post-depositional phenomena (sublimation and/or diffusion) in the snow cover of coastal Dronning Maud Land. Earlier cores drilled near Neumayer station (Table 1) also differ in mean  $d$  values with respect to snow. Firn core FB0202 (1981–2001) covers almost the same period as the fresh-snow samples (1981–2006). For this core, a lower average  $d$  value (5.5‰) was measured than for fresh snow (8.6‰). This  $d$  value is close to those of the firn cores from Halvfaryggen and Søråsen, implying that the dissimilarity in  $d$  values between fresh snow and firn cores is not produced by primary conditions of the snow, such as evaporation or condensation conditions. Vapour diffusion in the snow column has been reported by Schlosser and Oerter (2002b) at the Ekström Ice Shelf, producing a smoothing of the isotope signal due to isotopic redistribution by diffusion in the snow column. The high-resolution isotope measurements of cores FB0701 and FB0703 (retrieved at the same geographical position as FB0702 and B39, respectively) show a clear decrease in  $d$

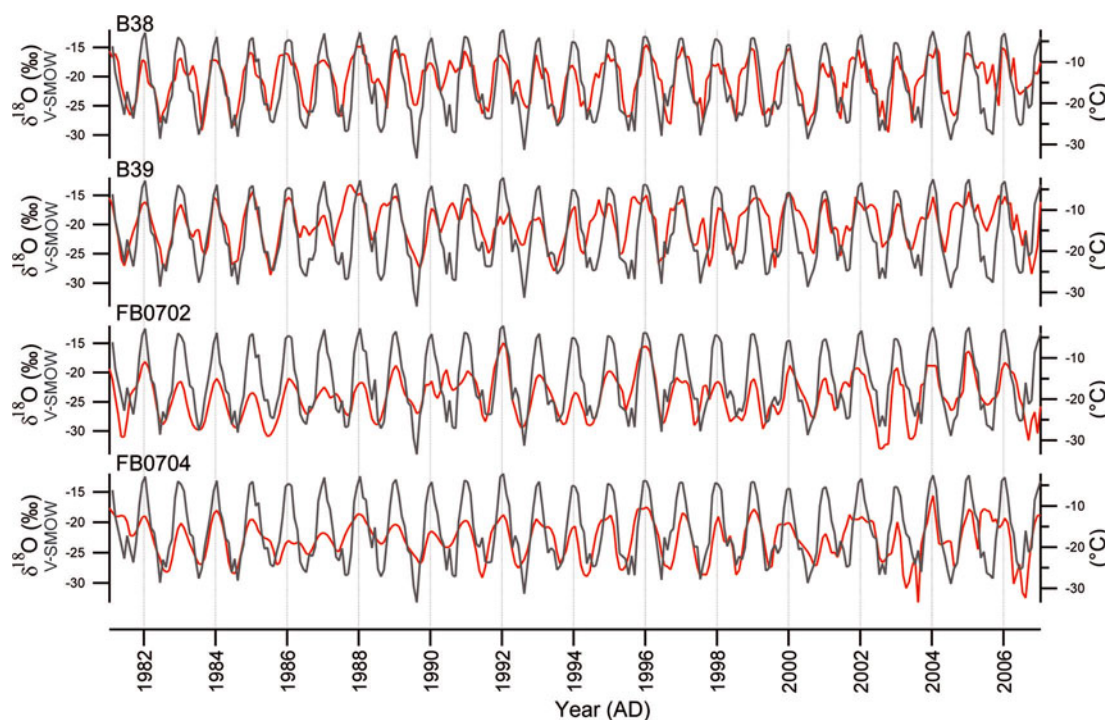


**Fig. 9.** Comparison of mean monthly air-temperature composite at Neumayer station (grey curves) and the high-resolution  $\delta^{18}\text{O}$  seasonal cycles (red curves).

with depth ( $-0.19\text{‰ m}^{-1}$  and  $-0.34\text{‰ m}^{-1}$ , respectively). These trends are attenuated in the related longer cores at Halvfarryggen (FB0702,  $-0.009\text{‰ m}^{-1}$ ) or even positive at Søråsen (B39,  $0.019\text{‰ m}^{-1}$ ), reinforcing the assumption of post-depositional processes in the upper firn layers. Removal and isotopic modification by sublimation cannot be discounted as a cause of the  $d$  variation. Based on an extensive database, Masson-Delmotte and others (2008) pointed out that mass loss caused by sublimation in low-elevation areas of Antarctica ( $<2400$  m a.s.l.) could lead to a decrease in  $d$  values. Ablation leads to longer exposure of the snow to the atmosphere, facilitating isotopic remobilization and fractionation. However, sublimation is likely not to be preponderant in the snow column, since no great differences in the co-isotope slope are detected, as expected for strong sublimation (Satake and Kawada, 1997; Zhou and others, 2008).

Histograms presented in Figure 8 demonstrate a common pattern of the distribution of  $d$  values for cores B39 and FB0704 from Søråsen and B38 from Halvfarryggen (mean  $d=6.5\text{‰}$ ,  $6.1\text{‰}$  and  $6.9\text{‰}$ , respectively). On the other hand, FB0702 (Halvfarryggen) shows a slightly lower  $d$  value

(mean  $d=5.4\text{‰}$ ). This likely reflects an additional moisture influence in core FB0702, which is in agreement with the interpretation of its  $\delta$  values.

## DISCUSSION

### $\delta^{18}\text{O}$ -temperature relationship

To investigate the relationship between stable-isotope composition and air temperatures, we compare monthly averages of air temperature at Neumayer station (1981–2007) with the  $\delta^{18}\text{O}$  annual cycles from firn cores (B38, B39, FB0702 and FB0704) to explain the variance of the water isotope composition (Fig. 9). High-resolution  $\delta^{18}\text{O}$  values were resampled to a monthly scale. We used a linear interpolation function of the seasonal isotope curves, assuming evenly distributed snowfall events throughout the year. In spite of the distance of the drilling sites from the stations, the air-temperature oscillations explain up to 50% (coefficient of determination,  $r^2$ ) of the  $\delta^{18}\text{O}$  variations (Fig. 10a–d); this relationship reaches its lowest values (30%) within core B39.

**Table 2.** Summary of stable water-isotope data of fresh-snow samples collected at Neumayer station from 1981 to 2006. In the rightmost column, slopes and intercepts of the calculated LMWL are presented. Coordinates and altitudes refer to WGS84

GvN		$\delta^{18}\text{O}$	$\delta\text{D}$	$d$	LMWL	
Coordinates	70.62° S, 8.37° W	‰	‰	‰		
Altitude	35 m a.s.l.					
Sampling period	1981–92					
		<b>Mean</b>	<b>-20.54</b>	<b>-156.3</b>	<b>8.6</b>	$\delta\text{D vs } \delta^{18}\text{O}$ slope: 7.95
		Std dev.	6.64	53.3	5.4	
		Min.	-39.88	-310.6	-4.8	
<i>Neumayer II</i>		Max.	-6.70	-48.3	28.9	$\delta\text{D vs } \delta^{18}\text{O}$ intercept: 7.60
Coordinates	70.65° S, 8.25° W					
Altitude	42 m a.s.l.					
Sampling period	1992–2006	$n$ (samples)	396	383	383	

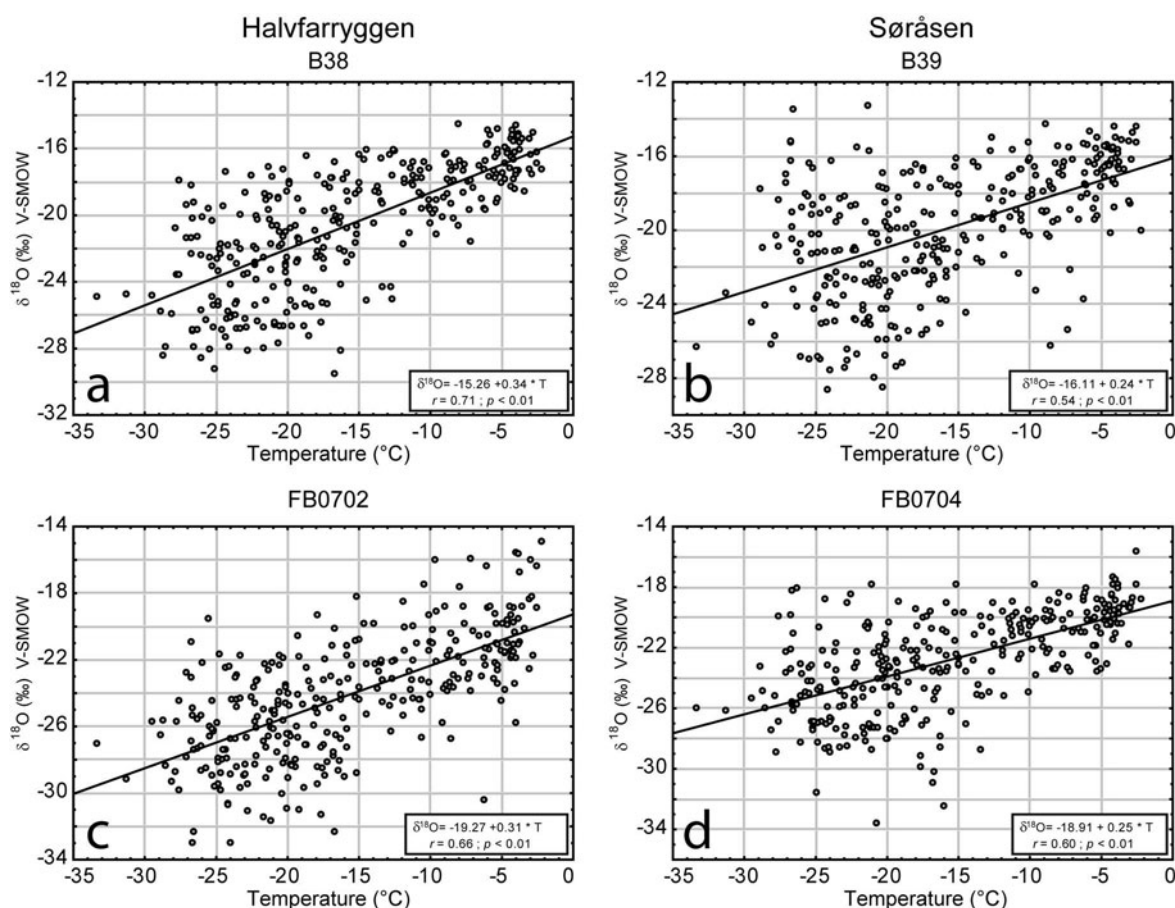


**Fig. 10.** Correlation of resampled mean  $\delta^{18}\text{O}$  values (12 per year) from firn cores (a) B38, (b) B39, (c) FB0702 and (d) FB0704 to monthly mean air temperature at Neumayer station. Correlation coefficients and statistical significance levels are displayed for all linear regressions.

For fresh-snow samples collected at Neumayer station (Fig. 11), as well as for all four firn cores (Fig. 10), a positive correlation between isotope composition and air temperature is evident. Air temperatures at the 2 m level explain 47% of the  $\delta^{18}\text{O}$  variation ( $r^2$ ). We conclude that both archives (firn cores and fresh snow) are good indicators of the regional climatological conditions and especially linked to variations of air temperatures.

A gradient of the  $\delta^{18}\text{O}$ –temperature relationship is noticeable between the ridges, with values of about 0.34–0.31‰ °C<sup>-1</sup> for Halvfarryggen and about 0.25‰ °C<sup>-1</sup> for Søråsen. In order to investigate whether this gradient is caused by post-depositional processes, we compared the

isotope/temperature slopes for both  $\delta^{18}\text{O}$  and  $\delta\text{D}$  on the shallow firn cores FB0701 (same position as FB0702) and FB0703 (same location as B39), following the same procedure as described earlier for the longer cores. The snow/firn contained in the shorter cores was exposed for a shorter time to local environmental conditions, so it should be less affected by possible post-depositional effects. Nevertheless, for both cores the slopes are similar to those at the same position, i.e. 0.36‰ °C<sup>-1</sup> for FB0701 (Halvfarryggen) and 0.18‰ °C<sup>-1</sup> for FB0703 (Søråsen) for  $^{18}\text{O}$ . The deuterium/temperature slopes are practically identical (multiplied by a factor of 8) to the oxygen slopes: 2.94‰ °C<sup>-1</sup> for FB0701 and 1.35‰ °C<sup>-1</sup> for FB0703. This

**Table 3.** Correlation matrix illustrating statistically significant correlation coefficients,  $r$ , between the  $\delta^{18}\text{O}$  values of cores B38, B39, FB0702 and FB0704. An increase in correlation coefficients is observed in the smoothed data. Strong correlation between the pairs B38–B39 and FB0702–FB0704 is obtained in both cases (smoothed and not smoothed). In the rightmost column, a significant temporal trend is found for core B39 (time interval 1962–2006). All statistically significant values are at  $p < 0.05$

	Mean acc. weighted $\delta^{18}\text{O}$ values				Smoothed mean $\delta^{18}\text{O}$ values				Year
	B38	B39	FB0702	FB0704	B38	B39	FB0702	FB0704	
B38	1.00	0.43	–	–	1.00	0.57	0.36	0.34	–
B39		1.00	0.34	–		1.00	0.30	–	0.32
FB0702			1.00	0.31			1.00	0.57	–
FB0704				1.00				1.00	–

confirms that the difference between the ridges is most likely a depositional phenomenon, dependent on the original stable-isotope composition of precipitation.

Helsen and others (2005) investigated the relationship between stable isotopes and local temperature in the neighbouring area of the Riiser-Larsen Ice Shelf, using an altitude profile from sea level to 2892 m a.s.l. (Kohnen station). They reported important differences between coastal and high-elevation areas. In coastal zones, the snowfall events are well distributed throughout the year. In contrast, snowfall events in higher areas occur preferentially in winter, associated with cyclonic activity. Additionally, the difference between 2 m air temperatures and condensation temperatures increases with the elevation of the area due to dominant air-temperature inversion in higher regions. This leads to an important seasonal and thermal bias in the interpretation of  $\delta^{18}\text{O}$  as a direct indicator of 2 m air-temperature variations. A similar difference in the temperature/isotope gradients was identified by Oerter and others (1999), comparing shallow firn cores and 10 m borehole temperatures. They concluded that the isotope-temperature relationship at the Ekström Ice Shelf ( $1.20\text{‰ }^{\circ}\text{C}^{-1}$  for  $\delta^{18}\text{O}$ ) decreases with increasing height towards the Amundsenisen plateau ( $0.69\text{‰ }^{\circ}\text{C}^{-1}$ ). Correct interpretation of the temperature-isotope relationship should take these factors into account. Low-altitude zones like Halvfarryggen and Søråsen are therefore better suited for an easier interpretation of the climatic signal contained in the isotope composition at a seasonal to sub-seasonal scale.

### Temporal stable-isotope trends

As previously demonstrated, the isotopic composition of the firn cores from both ridges (Halvfarryggen and Søråsen) reflects relatively well the meteorological conditions of the southern hinterland of the Ekström Ice Shelf. However, the correlation between the different stable-isotope datasets for our study region has not yet been explored.

With the aim of finding possible regional signals during the common time interval 1962–2006, a  $\delta^{18}\text{O}$  anomaly index ( $\Delta^{18}\text{O}$ ) was calculated to compare the firn cores on a common temporal scale. This index also allows removal of the isotopic effects (altitudinal and continental) and accumulation gradients from each individual dataset (different cores), since the index refers to the average value for each core and not to absolute  $\delta^{18}\text{O}$  values. The anomaly index was calculated by subtracting the accumulation-weighted  $\delta^{18}\text{O}$  average (1962–2006) from annual mean values (Fig. 12a). A correlation matrix of  $\delta^{18}\text{O}$  (Table 3) shows a good correlation of annual  $\delta^{18}\text{O}$  mean values between cores B38 and B39 ( $r=0.43$ ). This correlation decreases further inland towards cores FB0702 and FB0704 ( $r=0.31$ ). However, a high interannual variability was detected ( $\sigma=1.12\text{‰}$  and  $1.46\text{‰}$  in B38 and FB0702, respectively). Thereafter, annual oxygen isotope values were smoothed using a 5 year running average function, leading to further improvement of the correlation between the cores.

In Figure 12a, positive (red colours) and negative (blue colours) phases of the smoothed  $\Delta^{18}\text{O}$  index are displayed. The correlation matrix of the smoothed data demonstrates a statistically significant temporal correlation (at level  $p<0.05$ ) between B38, B39, FB0702 and FB0704 for the period 1962–2006. However, B39 does not correlate with FB0704. The strongest correlation is observed between the northern cores B38 and B39 as well as the hinterland cores FB0702 and

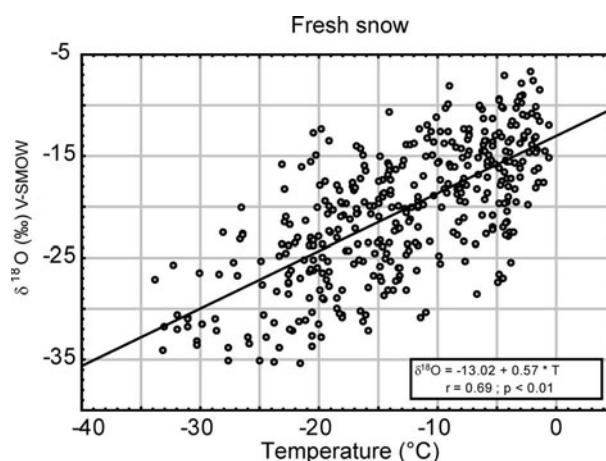


**Fig. 11.** Correlation of  $\delta^{18}\text{O}$  values from fresh-snow samples against air temperature. Snow samples were collected at Neumayer station during the years 1981–2006.

FB0704 ( $r=0.57$  for both pairs). Consequently, common 'positive' (warm) or 'negative' (cold) phases are evident for the firn cores (Fig. 12a). A common positive  $\Delta^{18}\text{O}$  index is likely found between 1975 and 1980 (prior to the meteorological records). However, the maximum peaks during this phase do not coincide in time and vary from about 1976 for B38, 1978 for B39 and FB0702, and 1979 for FB0704. This positive phase is followed by a less apparent negative phase, also showing a lag on the minimum peaks. Additionally, the  $\Delta^{18}\text{O}$  index of all cores shows a rather positive phase at about 2005 and a negative phase at about 1965.

Temporal trends were calculated for all firn cores using linear regressions from smoothed  $\Delta^{18}\text{O}$  time series (Fig. 12b). Using this parameter, no statistically significant trend (at  $p<0.05$ ) in the common time-span was found for cores B38, FB0702 and FB0704. In contrast, core B39 shows a slight positive trend (Fig. 9b).

Borehole temperature profiles (Fig. 13) measured 1 day after the drilling also show a slight decrease in temperature with depth, thus reinforcing our observations, and are coincident with our isotope data. Unfortunately, temperature trends cannot be precisely estimated because of possible remaining heat in the holes after the drilling. Temperatures decrease by  $0.006\text{--}0.013^{\circ}\text{C m}^{-1}$ . The profile of FB0704 is not shown because the temperature at this borehole was measured <24 hours after the drilling.

### Temporal and spatial variation of $d$

The temporal variation of  $d$  could reflect changes of the atmospheric circulation system in this region. This possibility was examined as for  $\delta^{18}\text{O}$  using linear regressions. Since the  $d$  values were calculated from low-resolution measurements it is not possible to calculate an exact annual mean value. In general, both coastal cores (B38 and B39) present statistically significant temporal variations in the secondary parameter  $d$ . However, the trends for both ridges are of the opposite sign. Halvfarryggen exhibits  $-0.04\text{‰ a}^{-1}$  variation of  $d$  and Søråsen  $+0.04\text{‰ a}^{-1}$ ; both slopes are moderate. For the inland cores FB0702 and FB0704, no statistically significant temporal trends were found; only minor trends ( $0.01\text{‰ a}^{-1}$ ) concordant in sign with those of the coastal region were observed. However, the influence of post-depositional effects on the  $d$  trends (e.g. diffusion) cannot be neglected completely. This

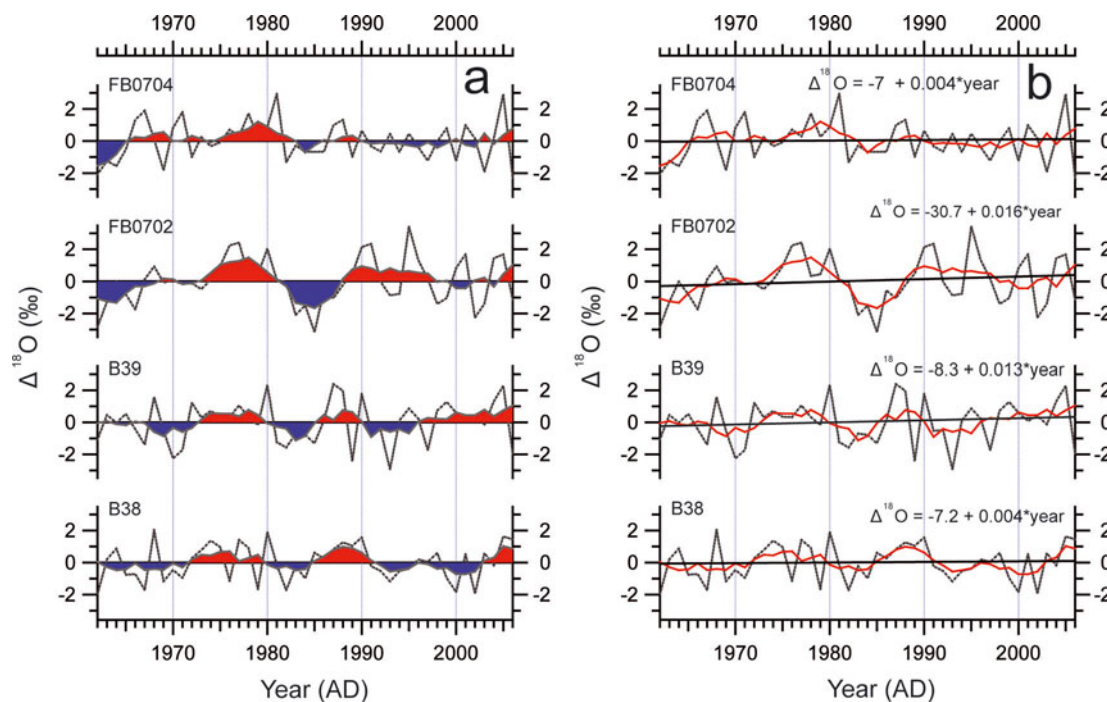


**Fig. 12.** (a)  $\delta^{18}\text{O}$  anomaly ( $\Delta^{18}\text{O}$ ) index (dashed grey line). Values were obtained by subtracting the accumulation-weighted annual  $\delta^{18}\text{O}$  average from single annual  $\delta^{18}\text{O}$  values. 5 year running head mean smoothed  $\Delta^{18}\text{O}$  is shown as a bold grey line. Positive (red areas) and negative (blue areas) smoothed index values are displayed to illustrate the correlation in time between the isotope data of the cores. Middle black line shows the mean accumulation-weighted  $\delta^{18}\text{O}$  average (zero line). (b) Linear regressions calculated for the anomaly indices of (a). Smoothed index is shown as a bold red line. For every core, linear regression lines are shown. No statistically significant trends ( $p < 0.05$ ) were found, except for core B39, which shows a positive tendency of  $0.013\text{‰ }^{18}\text{O a}^{-1}$  ( $r = 0.32$ ).

effect is restricted only to the first metres of firm, as determined by Schlosser and Oerter (2002a). Diffusion ceases to be important when the critical density of  $550 \text{ kg m}^{-3}$  is reached. In our cores this density is reached between 8 and 10 m depth for the north- and southward cores,

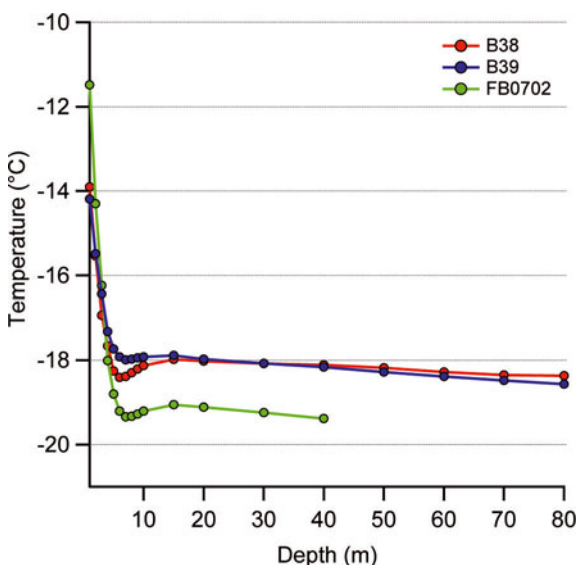


**Fig. 13.** Borehole temperature profiles for cores B38, B39 and FB0702. All profiles show a slightly decreasing temperature with depth. Temperatures were measured every metre for the first 10 m, every 5 m between 10 and 20 m depth and every 10 m between 20 m depth and the bottom of the hole. The profile of core FB0704 has been excluded because of signs of remaining heat influence.

respectively. If trends for both cores are calculated outside the diffusion zone, they are still present and preserve their sign. The trend for B38 is then statistically significant at  $p < 0.1$ . This observation could reveal a local variation of moisture transported to both ridges, although post-depositional effects cannot be excluded.

During the polynya periods 1974–76 and 1997–98, the  $d$  profiles display slightly higher values ( $d = 8\text{--}10\text{‰}$ ) than the mean  $d$  value of the cores. This could point to the addition of moisture from a local source region (with lower humidity and/or higher SST than the main moisture source; Uemura and others, 2008). According to Moore and others (2002), the SST had been significantly higher in polynya years, which would support the hypothesis of local moisture addition.

The reconstruction of moisture sources of accumulated precipitation within the recovered firm cores is difficult. In general, lower  $d$  values have been related to higher  $h$  and lower SST at the moisture source (Dansgaard, 1964; Clark and Fritz, 1997). Thus, it can be interpreted that the dominating moisture source of precipitation at Halvfaryggen and Søråsen should have a higher humidity and/or lower SST than the global average, since the GMWL is defined with a  $d$  value of  $10\text{‰}$ .

Schlosser and others (2008) reconstructed the source of snow precipitated at Neumayer station (between 1981 and 2000) based on combined backward trajectory computation and stable-isotope analysis. They found that the two most common atmospheric circulation paths arriving at the Ekström Ice Shelf originate either from the Weddell Sea or from the coastal east. In both source regions,  $d$  values are about  $9\text{‰}$ . Other frequent paths with different  $d$  values were also identified, but only oceanic moisture sources from relatively low latitudes (north of  $62^\circ \text{S}$ ) are able to produce a

low  $d$  value of 6–7‰ in this area. Uemura and others (2008) demonstrated a great variability of  $d$  in the coastal zone of East Antarctica, analysing water vapour collected directly above the sea surface. The  $d$  values were found to fluctuate between –5‰ and +18‰ as a consequence of moisture mixing from continental and oceanic sources. Based on similar variations in our study area (Fig. 8), a mixture of air masses from different moisture sources is indicated by our data, with a common signal for the whole region. The relatively coarse resolution of our measurements, as well as post-depositional effects, should be taken into account. Masson-Delmotte and others (2008) studied the geographical distribution of  $d$  values around Antarctica, demonstrating that in low-altitude coastal areas (<2000 m a.s.l.) the variation of  $d$  is mainly linked to regional conditions (moisture source). They demonstrated, in general, relatively low  $d$  values for coastal Antarctica (about 5‰ average) and higher values for the whole dataset (7.8‰). Our data correspond well to Antarctic mean  $d$  values, but exceed the observed coastal average values.

## CONCLUSIONS

Four firn cores were retrieved in January 2007 at Halvfarryggen and Søråsen in the coastal area of Dronning Maud Land, in order to study recent climate variability in this region by stable-isotope methods. These studies provide time series dating back to at least 1960. Different proxies indicate that the four cores reflect not only regional conditions but also local features, as demonstrated for example by the influence of the Weddell Sea polynya events (DEP,  $d$  and accumulation profiles).

Our studies demonstrate a statistically representative dependency of the water isotope composition at coastal Dronning Maud Land on precipitation and air temperatures registered at Neumayer station. The correlation between the isotopic composition of fresh-snow samples at Neumayer station and air temperature is high ( $r=0.69$ ), but no statistically significant temporal trend was found. This corresponds well with the findings of the data from firn cores and air temperatures. The best correlation between the isotopic composition of firn cores and air temperature at Neumayer station was found with respect to monthly means ( $r=0.54$ – $0.71$  in B39 and B38, respectively). The gradient in the  $\delta^{18}\text{O}$ –air-temperature relationship between Søråsen and Halvfarryggen ridges is evident. On Halvfarryggen (east ridge) the variation of air temperature explains the seasonal isotopic composition of firn from 43% (FB0702) up to 50% (B38) with an isotope/temperature gradient of  $0.33\text{‰ }^{\circ}\text{C}^{-1}$ . The relationship between  $\delta^{18}\text{O}$  and air temperature decreases to 29% (B39) and 35% (FB0704), and a lower gradient of  $0.25\text{‰ }^{\circ}\text{C}^{-1}$  at Søråsen (west ridge) is observed. Independent of spatial variations, no important temporal trends of  $\delta^{18}\text{O}$  are found for the firn cores or for fresh snow. Only B39 (Søråsen) shows a slight (and statistically significant) increase of  $0.013\text{‰ a}^{-1}$ , corresponding to an increase in air temperatures of about  $0.6^{\circ}\text{C}$  between 1962 and 2006. At Halvfarryggen (B38 and FB0704) no significant temperature trend is visible for this period. As a consequence, no general warming (or cooling) trend can be inferred for the last half-century. This conclusion agrees with MAAT data from Neumayer station, where annual temperatures for the period 1981–2006 show no trend, with an average of  $-16.1^{\circ}\text{C}$  (König-Langlo and Loose, 2007).

The strong correlation of  $\delta^{18}\text{O}$  variations between the firn cores in the hinterland of Neumayer station allows us to conclude that condensation conditions of the precipitation are similar for the whole coastal region. The isotope fractionation process changes at  $\sim 700$  m a.s.l., above which isotope altitude effects are detected (visible only in core FB0704). Similar conclusions were made by Helsen and others (2006), who identified the beginning of altitudinal fractionation processes at coastal Dronning Maud Land during uplift and cooling of moist masses when confronting the Antarctic continent. The  $\delta^{18}\text{O}$  values of their snow pits at 1160 m a.s.l. (–30.4‰) are clearly depleted with respect to coastal values (–21.4‰ to –23.3‰).

Spatial differences between the ridges are observed with regard to their respective accumulation rates (as for  $\delta^{18}\text{O}$  values), especially at the firn cores closer to the coast. The accumulation rates of  $1257\text{ kg m}^{-2}\text{ a}^{-1}$  on Halvfarryggen (B38) are higher than those of  $818\text{ kg m}^{-2}\text{ a}^{-1}$  on Søråsen (B39). Towards the hinterland, a decrease in accumulation rates to about  $500\text{ kg m}^{-2}\text{ a}^{-1}$  is observed for both inland cores (FB0702 and FB0704). However, FB0702 is probably influenced by snowdrift from higher altitudes and/or erosion, as demonstrated by its relatively low  $\delta^{18}\text{O}$  values.

The spatial variations of accumulation rates,  $d$  values and the isotope/temperature relationship are likely to be linked to the wind regime and transport of moisture masses. The easterly wind, as the dominant regional wind regime, carries mixed oceanic moisture influenced by humidity of continental origin. The oceanic input over Halvfarryggen seems to have increased in the past half-century, evidenced by the negative temporal trend of  $d$  values for both cores of this ridge (although statistically not significant for FB0702). An opposite tendency (positive sign) is found for Søråsen. There is no obvious explanation for these trends, since both ridges are under the influence of the same regional climate. Trends of  $d$  values could either represent variations of the regional wind regime or be a product of post-depositional effects acting over the snow column. Relatively moist air masses first confront Halvfarryggen (east ridge). This ridge then probably acts as a natural barrier blocking the passage of moisture to the west, thus producing a ‘shadowing effect’.

The summits of both Halvfarryggen and Søråsen are sites with high accumulation rates and thus might be suitable locations for deep drilling, due also to the appropriate geographical and ice conditions (ice thickness, MAAT, geographical location). Since the ice cover could reach 800 m thickness or more in this area (Steinhage and others, 1999), the future drill site could reveal a high-resolution climate record of the atmospheric temperature evolution for at least the past 1.9 ka.

## ACKNOWLEDGEMENTS

We thank the international team who carried out the fieldwork and later performed the laboratory measurements. P. Kaufmann (University of Bern), M. Bock, C. Wesche, D. Steinhage (AWI) and M. Blattner (Kässbohrer company) carried out the fieldwork in Antarctica. The borehole thermistor probe was provided by the Centre for Ice and Climate, University of Copenhagen. S. Kipfstuhl and F. Valero were in charge of the AWI cold laboratory during the ice-core processing. Y. Schlomann, G. Meyer, L. Schöncke and E. Nebel (AWI) performed the stable-isotope measurements and P. Seibel (Helmholtz-Zentrum München) carried out the

tritium measurements. T. Opel is thanked for fruitful discussions. We thank E. Isaksson and an anonymous reviewer for their comments which improved the manuscript. The PhD fellowship awarded to F. Fernandoy by the German Academic Exchange Service (DAAD) is gratefully acknowledged.

## REFERENCES

- Ackley, S.F., C.A. Geiger, J.C. King, E.C. Hunke and J. Comiso. 2001. The Ronne polynya of 1997/98: observations of air–ice–ocean interaction. *Ann. Glaciol.*, **33**, 425–429.
- Bertler, N.A.N. and 53 others. 2005. Snow chemistry across Antarctica. *Ann. Glaciol.*, **41**, 167–179.
- Brook, E.J., E. Wolff, D. Dahl-Jensen, H. Fischer and E.J. Steig. 2006. The future of ice coring: International Partnerships in Ice Core Sciences (IPICS). *PAGES News*, **14**(1), 6–10.
- Carsey, F.D. 1980. Microwave observations of the Weddell polynya. *Mon. Weather Rev.*, **108**(1), 2032–2044.
- Chapman, W.L. and J.E. Walsh. 2007. A synthesis of Antarctic temperatures. *J. Climate*, **20**(16), 4096–4117.
- Chen, J.L., C.R. Wilson, D. Blankenship and B.D. Tapley. 2009. Accelerated Antarctic ice loss from satellite gravity measurements. *Nature Geosci.*, **2**(12), 859–862.
- Clark, I.D. and P. Fritz. 1997. *Environmental isotopes in hydrogeology*. Boca Raton, FL, CRC Lewis.
- Craig, H. 1961. Isotopic variations in meteoric waters. *Science*, **133**(3465), 1702–1703.
- Dansgaard, W. 1964. Stable isotopes in precipitation. *Tellus*, **16**(4), 436–468.
- Davis, C.H., Y. Li, J.R. McConnell, M.M. Frey and E. Hanna. 2005. Snowfall-driven growth in East Antarctic ice sheet mitigates recent sea-level rise. *Science*, **308**(5730), 1898–1901.
- De Angelis, H. and P. Skvarca. 2003. Glacier surge after ice shelf collapse. *Science*, **299**(5612), 1560–1562.
- Eisen, O. and 15 others. 2008. Ground-based measurements of spatial and temporal variability of snow accumulation in East Antarctica. *Rev. Geophys.*, **46**(RG2), RG2001. (10.1029/2006RG000218.)
- EPICA Community Members. 2004. Eight glacial cycles from an Antarctic ice core. *Nature*, **429**(6992), 623–628.
- EPICA Community Members. 2006. One-to-one coupling of glacial climate variability in Greenland and Antarctica. *Nature*, **444**(7116), 195–198.
- Gillett, N.P. and 7 others. 2008. Attribution of polar warming to human influence. *Nature Geosci.*, **1**(11), 750–754.
- Helsen, M.M., R.S.W. van de Wal, M.R. van den Broeke, D. van As, H.A.J. Meijer and C.H. Reijmer. 2005. Oxygen isotope variability in snow from western Dronning Maud Land, Antarctica and its relation to temperature. *Tellus*, **57B**(5), 423–435.
- Helsen, M.M. and 6 others. 2006. Modeling the isotopic composition of Antarctic snow using backward trajectories: simulation of snow pit records. *J. Geophys. Res.*, **111**(D15), D15109. (10.1029/2005JD006524.)
- Hofstede, C.M. and 10 others. 2004. Firn accumulation records for the past 1000 years on the basis of dielectric profiling of six cores from Dronning Maud Land, Antarctica. *J. Glaciol.*, **50**(169), 279–291.
- Holland, D.M. 2001. Explaining the Weddell Polynya – a large ocean eddy shed at Maud Rise. *Science*, **292**(5522), 1697–1700.
- Jouzel, J. and L. Merlivat. 1984. Deuterium and oxygen 18 in precipitation: modeling of the isotopic effect during snow formation. *J. Geophys. Res.*, **89**(D7), 11,749–11,757.
- Jouzel, J. and 31 others. 2007. Orbital and millennial Antarctic climate variability over the past 800,000 years. *Science*, **317**(5839), 793–796.
- König-Langlo, G. and B. Loose. 2007. The meteorological observatory at Neumayer Stations (GvN and NM-II) Antarctica. *Polarforschung*, **76**(1–2), 25–38.
- Levitus, S., J.I. Antonov, T.P. Boyer and C. Stephens. 2000. Warming of the world ocean. *Science*, **287**(5461), 2225–2229.
- Marshall, G.J. 2007. Half-century seasonal relationships between the Southern Annular mode and Antarctic temperatures. *Int. J. Climatol.*, **27**(3), 373–383.
- Marshall, G.J., A. Orr and N.P.M. van Lipzig. 2006. The impact of a changing Southern Hemisphere annular mode on Antarctic Peninsula summer temperatures. *J. Climate*, **19**(20), 5388–5404.
- Masson-Delmotte, V. and 35 others. 2008. A review of Antarctic surface snow isotopic composition: observations, atmospheric circulation, and isotopic modeling. *J. Climate*, **21**(13), 3359–3387.
- Merlivat, L. and J. Jouzel. 1979. Global climatic interpretation of the deuterium–oxygen 18 relationship for precipitation. *J. Geophys. Res.*, **84**(C8), 5029–5033.
- Meyer, H., L. Schönicke, U. Wand, H.W. Hubberten and H. Friedrichsen. 2000. Isotope studies of hydrogen and oxygen in ground ice: experiences with the equilibration technique. *Isot. Environ. Health Stud.*, **36**(2), 133–149.
- Monaghan, A.J., D.H. Bromwich, W. Chapman and J.C. Comiso. 2008. Recent variability and trends of Antarctic near-surface temperature. *J. Geophys. Res.*, **113**(D4), D04105. (10.1029/2007JD009094.)
- Moore, G.W.K., K. Alverson and I.A. Renfrew. 2002. A reconstruction of the air–sea interaction associated with the Weddell polynya. *J. Phys. Oceanogr.*, **32**(6), 1685–1698.
- Oerter, H., W. Graf, F. Wilhelms, A. Minikin and H. Miller. 1999. Accumulation studies on Amundsenisen, Dronning Maud Land, by means of tritium, dielectric profiling and stable-isotope measurements: first results from the 1995–96 and 1996–97 field seasons. *Ann. Glaciol.*, **29**, 1–9.
- Rignot, E. 2006. Changes in ice dynamics and mass balance of the Antarctic ice sheet. *Philos. Trans. R. Soc. London, Ser. A*, **364**(1844), 1637–1655.
- Rignot, E. and R.H. Thomas. 2002. Mass balance of polar ice sheets. *Science*, **297**(5586), 1502–1506.
- Rignot, E., G. Casassa, P. Gogineni, W. Krabill, A. Rivera and R. Thomas. 2004. Accelerated ice discharge from the Antarctic Peninsula following the collapse of Larsen B ice shelf. *Geophys. Res. Lett.*, **31**(18), L18401. (10.1029/2004GL020697.)
- Robertson, R., M. Visbeck, A.L. Gordon and E. Fahrbach. 2002. Long-term temperature trends in the deep waters of the Weddell Sea. *Deep-Sea Res. II*, **49**(21), 4791–4806.
- Rotschky, G. and 6 others. 2007. A new surface accumulation map for western Dronning Maud Land, Antarctica, from interpolation of point measurements. *J. Glaciol.*, **53**(182), 385–398.
- Satake, H. and K. Kawada. 1997. The quantitative evaluation of sublimation and the estimation of original hydrogen and oxygen isotope ratios of a firn core at East Queen Maud Land, Antarctica. *Bull. Glacier Res.*, **15**, 93–97.
- Scambos, T.A., C. Hulbe, M. Fahnestock and J. Bohlander. 2000. The link between climate warming and break-up of ice shelves in the Antarctic Peninsula. *J. Glaciol.*, **46**(154), 516–530.
- Schlosser, E. and H. Oerter. 2002a. Seasonal variations of accumulation and the isotope record in ice cores: a study with surface snow samples and firn cores from Neumayer station, Antarctica. *Ann. Glaciol.*, **35**, 97–101.
- Schlosser, E. and H. Oerter. 2002b. Shallow firn cores from Neumayer, Ekströmis, Antarctica: a comparison of accumulation rates and stable-isotope ratios. *Ann. Glaciol.*, **35**, 91–96.
- Schlosser, E., C. Reijmer, H. Oerter and W. Graf. 2004. The influence of precipitation origin on the  $\delta^{18}\text{O}$ – $T$  relationship at Neumayer station, Ekströmis, Antarctica. *Ann. Glaciol.*, **39**, 41–48.
- Schlosser, E., H. Oerter, V. Masson-Delmotte and C. Reijmer. 2008. Atmospheric influence on the deuterium excess signal in polar firn: implications for ice-core interpretation. *J. Glaciol.*, **54**(184), 117–124.
- Schneider, D.P. and 6 others. 2006. Antarctic temperatures over the past two centuries from ice cores. *Geophys. Res. Lett.*, **33**(16), L16707. (10.1029/2006GL027057.)

- Sharp, Z. 2006. *Principles of stable isotope geochemistry*. Upper Saddle River, NJ, Prentice Hall.
- Shepherd, A., D. Wingham and E. Rignot. 2004. Warm ocean is eroding West Antarctic Ice Sheet. *Geophys. Res. Lett.*, **31**(23), L23404. (10.1029/2004GL021106.)
- Solomon, S. and 7 others, eds. 2007. *Climate change 2007: the physical science basis. Contribution of Working Group I to the Fourth Assessment Report of the Intergovernmental Panel on Climate Change*. Cambridge, etc., Cambridge University Press.
- Steig, E.J., D.P. Schneider, S.D. Rutherford, M.E. Mann, J.C. Comiso and D.T. Shindell. 2009. Warming of the Antarctic ice-sheet surface since the 1957 International Geophysical Year. *Nature*, **457**(7228), 459–462.
- Steinhage, D., U. Nixdorf, U. Meyer and H. Miller. 1999. New maps of the ice thickness and subglacial topography in Dronning Maud Land, Antarctica, determined by means of airborne radio-echo sounding. *Ann. Glaciol.*, **29**, 267–272.
- Thompson, D.W.J. and S. Solomon. 2002. Interpretation of recent Southern Hemisphere climate change. *Science*, **296**(5569), 895–899.
- Traufetter, F., H. Oerter, H. Fischer, R. Weller and H. Miller. 2004. Spatio-temporal variability in volcanic sulphate deposition over the past 2 kyr in snow pits and firn cores from Amundsenisen, Antarctica. *J. Glaciol.*, **50**(168), 137–146.
- Turner, J., T. Lachlan-Cope, S. Colwell and G.J. Marshall. 2005. A positive trend in western Antarctic Peninsula precipitation over the last 50 years reflecting regional and Antarctic-wide atmospheric circulation changes. *Ann. Glaciol.*, **41**, 85–91.
- Uemura, R., Y. Matsui, K. Yoshimura, H. Motoyama and N. Yoshida. 2008. Evidence of deuterium excess in water vapor as an indicator of ocean surface conditions. *J. Geophys. Res.*, **113**(D19), D19114. (10.1029/2008JD010209.)
- Van den Broeke, M.R. and N.P.M. van Lipzig. 2003. Factors controlling the near surface wind field in Antarctica. *Mon. Weather Rev.*, **131**(4), 733–743.
- Van den Broeke, M.R. and N.P.M. van Lipzig. 2004. Changes in Antarctic temperature, wind and precipitation in response to the Antarctic Oscillation. *Ann. Glaciol.*, **39**, 119–126.
- Van den Broeke, M.R., N.P.M. van Lipzig and E. van Meijgaard. 2002. Momentum budget of the East-Antarctic atmospheric boundary layer: results of a regional climate model. *J. Atmos. Sci.*, **59**(21), 3117–3129.
- Wesche, C., S. Riedel and D. Steinhage. 2009. Precise surface topography of the grounded ice ridges at the Ekströmisen, Antarctica, based on several geophysical data sets. *ISPRS J. Photogramm. Rem. Sens.*, **64**(4), 381–386.
- Wilhelms, F. 2000. Messung dielektrischer Eigenschaften polarer Eiskerne. *Ber. Polarforsch. Rep. Pol. Res.* 367.
- Wilhelms, F. 2005. Explaining the dielectric properties of firn as a density-and-conductivity mixed permittivity (DECOMP). *Geophys. Res. Lett.*, **32**(16), L16501. (10.1029/2005GL022808.)
- Zhou, S., M. Nakawo, S. Hashimoto and A. Sakai. 2008. The effect of refreezing on the isotopic composition of melting snowpack. *Hydrol. Process.*, **22**(6), 873–882.

MS received 23 December 2009 and accepted in revised form 12 June 2010